JOURNAL OF MATERIALS SCIENCE 37 (2002) 4801 – 4809

Effect of polyester structure on the interaction parameters and morphology development of ternary blends: Model for high performance adhesives and coatings

D. J. DUFFY, H. D. STIDHAM, S. L. HSU*
Polymer Science and Engineering Department and Chemistry Department, University of Massachusetts, Amherst, Massachusetts 01003, USA
E-mail: slhsu@polysci.umass.edu

SONO SASAKI, ATSUSHI TAKAHARA, TISATO KAJIYAMA
Department of Applied Chemistry, Kyushu University, Fukuoka, Japan

Studies were conducted on ternary blends consisting of poly(propylene oxide) and poly(methyl methacrylate co *n*-butyl methacrylate) blended with either poly(hexamethylene adipate) or poly(hexamethylene sebacate). These ternary blends form the basis for preparation of high performance polyurethane-based hot-melt adhesives and coatings. Changes in polyester structure were found to strongly alter the miscibility behavior. Binary interaction parameters for the five polymer pairs were determined experimentally, permitting calculation of the phase behavior of the ternary polymer blends. Results predicted by the model are in excellent agreement with experimental observations. The influence of miscibility in the melt on the morphology development is also discussed.

1. Introduction

Polyurethane possesses considerable advantages in performance over other types of adhesives and coatings. They have attractive properties, fast curing speed, and ideal mechanical properties. Generally, these systems involve reactions of highly fluid isocyanates and hydroxyl terminated polyethers to form prepolymers [1–3]. When applied to various surfaces, they react with moisture in the environment to form mechanical bonds. Blends are usually employed to alter or improve processing speed, raise viscosity (green strength) and physical properties [4, 5]. There is no fundamental study of the phase equilibria of such reactive systems nor of the influence of individual components on miscibility behavior. In the absence of such information, altering or finding new processing conditions or compositions is a non-trivial and unavoidable empirical task. The present work is directed at determining the molecular origins of miscibility in a ternary hot-melt polyurethane adhesive system, allowing some prediction and control of the phase behavior and blend morphology.

The blend given principal emphasis is composed of poly(propylene glycol), an aliphatic-polyester and an acrylic co-polymer. This system is simple enough for fundamental analysis yet sufficiently complex to represent commercial adhesive formulations. The polyether and polyester diols provide reactive functional groups for synthesis of urethane linkages. Copolymers are often added to enhance the miscibility of polyesters with the polyethers used in the formulation [4, 6]. The morphological features formed (polyester crystals) and the high T_g acrylic component provide considerable mechanical strength and processing control. Knowledge of phase behavior of these reactive components provides better understanding of how chemical reaction contributes to miscibility and morphology of the final system [7, 8].

Polymer miscibility stems from a balance between the enthalpic and entropic contributions to the free energy of mixing. There are numerous ways to modify this balance, and the number of possible polymer variations, interaction parameters and blend properties is enormous. The chemical structure of polymer repeat units [9, 10], copolymer composition [11], copolymer sequence distribution [8], polymer branching [12], tacticity [13], end groups [14], and hydrogen bond interactions [15, 16] have all been shown to contribute to polymer miscibility. Of these, the influence of the length of aliphatic chains on the miscibility of ternary blends that include these aliphatic chains was selected for the work here. This effect has been suggested to be important in binary blends of aliphatic polyesters with poly(vinyl chloride) [17], poly(epichlorohydrin) [18],

*Author to whom all correspondence should be addressed.

polyhydroxy ether of bisphenol-A [19] and tetramethyl bisphenol-A polyarylate [9].

Manipulation of the polymer properties listed above results in differences in segmental interactions between or within chains. Polymer–polymer interaction parameters or functions are typically used to quantify the thermodynamic behavior of polymer blends [20–22]. If interaction parameters are known, the phase behavior of a polymer mixture can be determined. A complete method does not yet exist for the prediction of interaction energies and polymer–polymer miscibility. Although predictive models based on group methods [23] and heats of mixing for small molecule analogues [24] have been developed, interaction parameters must still be determined experimentally for most systems. In the work reported here, phase equilibria of binary mixtures of the ternary components were determined and the interaction parameters obtained for the binary mixtures. The determined interaction parameters proved to have good predictive qualities when applied to ternary mixtures of the components. Morphological differences at different points in the phase diagram were also established. In this study we aim to provide insight into how the immiscible PPG/polyester pair can co-exist in the same phase by the addition of the third polymeric component and the influence of the polyester structure on the miscibility of this system. Our results are reported herein.

2. Experimental

Poly(propylene glycol) (PPG) has been obtained from ARCH Chemical; poly(hexamethylene adipate) (PHMA) and poly(hexamethylene sebacate) (PHMS) were obtained from Dow Chemical. A random copolymer resin of methyl methacrylate and *n*-butyl methacrylate [P(MMA*n*BMA)] was obtained from INEOS Acrylics. The molecular structure of the four components is shown in Fig. 1.

The molecular weight of poly(propylene oxide) and the two polyesters were determined using a Bruker Daltonics Reflex III, Matrix Assisted Laser Desorption Ionization Time of Flight (MALDI-TOF) mass spectrometer operating in the reflectron mode. Saturated dithranol in $CHCl_3$ and sodium tri-fluoroacetate (NaTFAc) in THF or MeOH (5 kg/m^3) were used as matrix and ionization agent solution, respectively. The molecular weight of P(MMA*n*BMA) was determined using GPC calibrated with PMMA standards in THF.

The acrylic copolymer composition was determined to be 0.75 and 0.25 mole fraction of MMA and *n*BMA, respectively, using NMR. Integration of the resonances

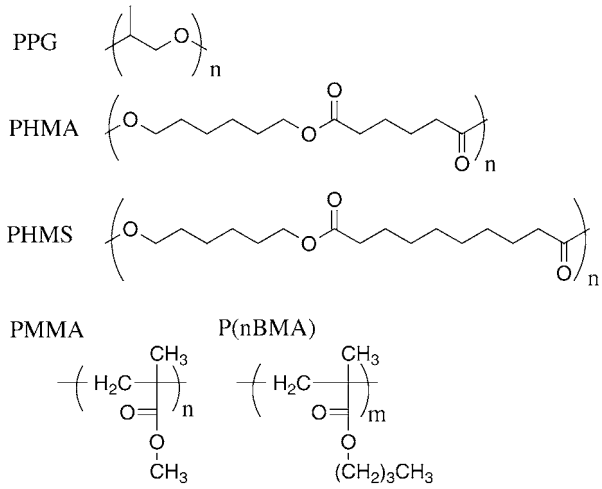

Figure 1 Chemical structures of polymers used in this investigation.

of methyl and methylene groups adjacent to the COO unit centered at 3.6 and 3.9 ppm can be used to define the ratio of MMA to *n*BMA in the copolymer [25]. All ^{1}H-NMR were recorded in $CDCl_3$ using a Bruker DPX300 spectrometer. Infrared spectra were obtained using a Perkin-Elmer 2000 Fourier transform infrared spectrometer equipped with a wide-band MCT detector in the transmission mode at 2 cm^{-1} resolution. The polymer films were cast from CH_2Cl_2 onto AgCl plates.

The molecular weight per repeat unit of P(MMA*n*BMA) is given by the weighted average of MMA and *n*BMA based on the copolymer composition. Densities were determined directly by displacement in the case of solids or using a pycnometer in the case of liquids. The densities of PHMA and PHMS are reported for solids at room temperature and in the melt at 120°C. Melting point depression measurements were performed using a TA Instruments DSC 2910, aluminum pans and a heating rate of 10°C/min. The enthalpy of fusion for PHMS was determined to be 92.03 J/g from thermal analysis. Glass transition temperature measurements were performed using a TA Instruments Q-1000 DSC. The physical data collected for the four polymers are presented in Table I.

Binary and ternary polymer blends were prepared in glass vials. The blends are placed in a vacuum oven at the melt temperature and allowed to equilibrate under vacuum to avoid decomposition. The oven was opened periodically and the blends mixed and vacuum reapplied. The physical appearance of many blends suggests the existence of multiple phases. A home-made microscope hot-stage cell coupled to a HeNe laser was constructed for determination of the overall transmission

TABLE I Physical property data

	M_w (g/mol)	M_w/M_n	ρ_{solid} (kg/m^3)	ρ_{liquid} (kg/m^3)	T_m (°C)	T_g (°C)	M_{repeat} (g/mol)	N_{repeat}	V_{repeat} (cm^3/mol)	n[a]
PPG	1906	1.01		1003	−30	−66	58	33	57.4	33
PHMA	2505	1.59	1158	1051	54.5	−61	228	11	216.2	44
PHMS	2194	1.60	1110	988	64.6	−60[b]	284	8	277.6	39
P(MMA*n*BMA)	30900	1.64	1150			85.3	110.5	280	95.9	468

[a]Degree of polymerization, with respect to Poly(propylene oxide) repeat unit volume.
[b]From [18].

of the sample. Micrographs of blends in the melt and at room temperature were recorded electronically using a VideoFlex 7300 digital camera and an Olympus Vanox optical microscope.

3. Results and discussions

3.1. Miscibility behavior and phase diagrams for ternary blends

The phase diagrams of ternary blends of poly(propylene glycol) (PPG), poly(hexamethylene adipate) (PHMA) or poly(hexamethylene sebacate) (PHMS), poly(methyl methacrylate co *n*-butyl methacrylate) [P(MMA*n*BMA)] are extremely fascinating as shown in Figs 2 and 3. Phase diagrams at 110 and 140°C were selected since they are consistent with the conditions needed for synthesis and application of polyurethane based hot-melt adhesives [2, 3]. The co-existence curves were previously determined using optical transmission experiments [26]. Following those studies and using the apparatus constructed in our laboratory, phase diagrams of ternary blends consisting of PPG, PHMS or PHMA, P(MMA*n*BMA) as determined by the optical appearance of the blends, are shown in Figs 2 and 3. Homogeneous blends have a uniform index of refraction and appear optically transparent. In contrast, heterogeneous systems have discontinuities in the refractive index causing an opaque or turbid appearance. Ternary blends of PPG, PHMA, and P(MMA*n*BMA) are composed of three partially miscible binary blends and display a region of miscibility near the center of Fig. 2. The boundary between the opaque and clear blends changes significantly with decreasing temperature. The addition of the acrylic copolymer of greater than 20% appears to promote compatibility of the polyether and polyester components leading to optically clear blends. The centrally located completely clear region

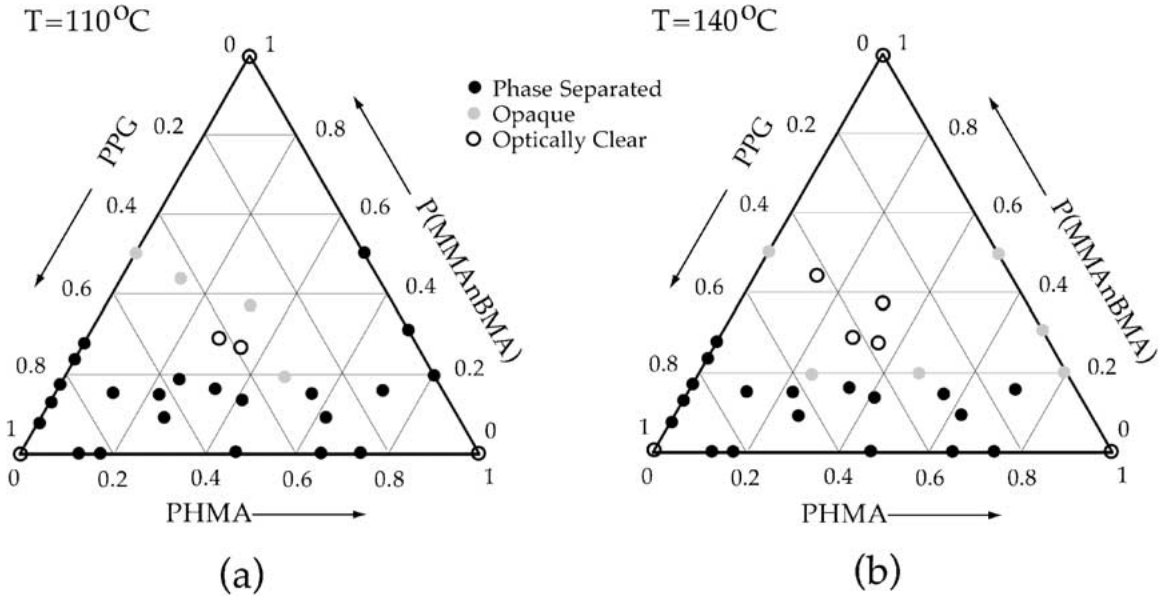

Figure 2 Miscibility diagram for ternary blends of PPG, PHMA and P(MMA*n*BMA) at (a) 110°C and (b) 140°C.

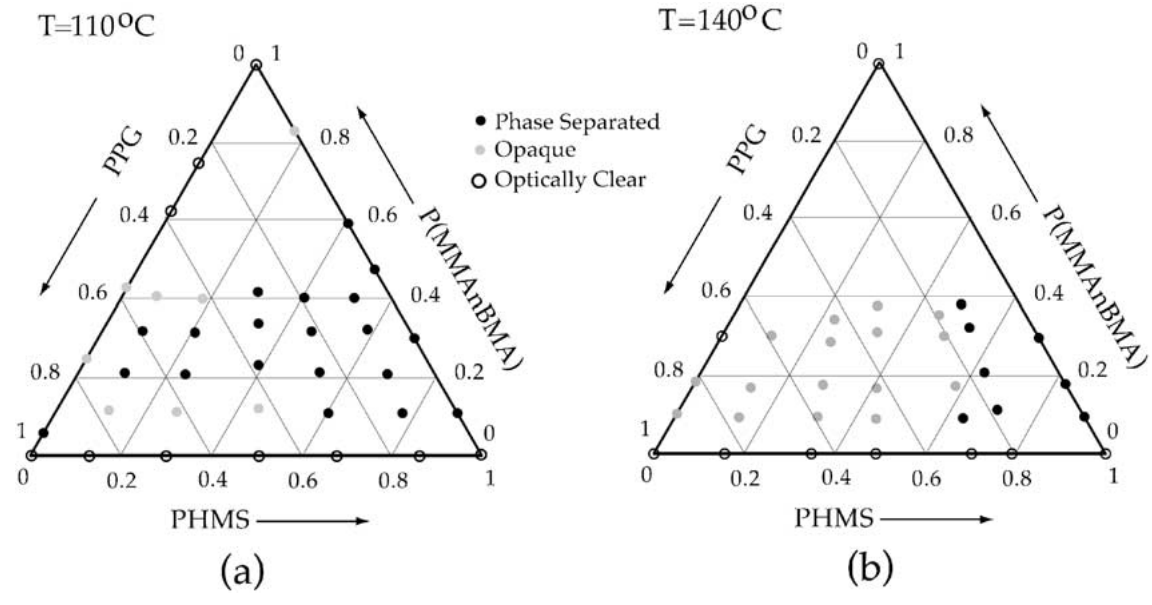

Figure 3 Miscibility diagram for ternary blends of PPG, PHMS and P(MMA*n*BMA) at (a) 110°C and (b) 140°C.

in Fig. 2a is interesting and "islands" of miscibility have been observed in other polymer systems. [27] We have no interpretation at this moment. Fig. 3 shows the miscibility phase diagram for ternary blends of PPG, PHMS, and P(MMA*n*BMA) at 110 and 140°C. In contrast to the first system, this ternary system is composed of two partially miscible and one miscible binary polymer pair. The PPG/PHMS binary is miscible whereas the PPG/PHMA binary is not. The consequence of the polyester structural change on the miscibility of the ternary blends is dramatic.

3.2. Thermodynamic analysis of binary and ternary blends

The thermodynamic treatment of phase behavior of polymer blends and solutions is well developed [11, 21, 26]. Determination of the binary interaction parameters and calculation of the phase diagrams is presented below. The free energy of mixing for strictly binary and ternary blends is given by Equations 1 and 2, respectively [20–22, 28, 29].

$$\frac{\Delta G^{\text{mix}}}{NRT} = \left(\frac{\phi_1 \ln(\phi_1)}{n_1} + \frac{\phi_2 \ln(\phi_2)}{n_2}\right) + (g_{1,2}\phi_1\phi_2) \quad (1)$$

$$\frac{\Delta G^{\text{mix}}}{NRT} = \left(\frac{\phi_1 \ln(\phi_1)}{n_1} + \frac{\phi_2 \ln(\phi_2)}{n_2} + \frac{\phi_3 \ln(\phi_3)}{n_3}\right) + (g_{1,2}\phi_1\phi_2) + (g_{1,3}\phi_1\phi_3) + (g_{2,3}\phi_2\phi_3) \quad (2)$$

where n_i is the degree of polymerization, ϕ_i is the volume fraction and the three g_{ij} values are binary interaction functions which may depend on composition and temperature [30]. Terms in the first bracket represent the entropic contribution to mixing, terms involving g_{ij} represent the enthalpic contribution. Only pairwise interaction terms are retained in Equations 1 and 2. Higher order interaction terms involving the product $(\phi_1\phi_2\phi_3)$ are occasionally retained to fit experimentally observed phase behavior in polymer solutions [31, 32]. It is known that molecular weight distribution needs to be considered for the analysis of the cloud point data of some polymer blends. [21, 30] We have not taken this aspect into account because of the excellent agreement found between experimental and calculated miscibility diagrams.

To directly determine thermodynamic interaction properties, we make use of the fact that fortuitously four out of five binary blends phase separate! The partitioning of mass between the two co-existing phases allows the chemical potential to be used to determine the binary interaction parameter. The measurement of the masses and compositions allows for application of the following analysis. Taking the appropriate derivatives of Equation 1 with respect to composition, Equations 3a and b can be obtained for the chemical potential of component 1 in co-existing phases I and II, respectively.

$$\frac{\Delta\mu_1^{\text{I}}}{RT} = \ln\left(\phi_1^{\text{I}}\right) - \phi_1^{\text{I}} - \frac{n_1}{n_2}\phi_2^{\text{I}} + n_1 g_{1,2}\left(\phi_2^{\text{I}}\right)^2 + 1 \quad (3a)$$

$$\frac{\Delta\mu_1^{\text{II}}}{RT} = \ln\left(\phi_1^{\text{II}}\right) - \phi_1^{\text{II}} - \frac{n_1}{n_2}\phi_2^{\text{II}} + n_1 g_{1,2}\left(\phi_2^{\text{II}}\right)^2 + 1 \quad (3b)$$

Equating (3a) and (3b) and after rearrangement, the interaction parameter g_{12} in terms of the composition of the two coexisting phases can be obtained.

$$g_{1,2} = \frac{\ln\left(\frac{\phi_1^{\text{I}}}{\phi_1^{\text{II}}}\right) + \left(\phi_1^{\text{II}} - \phi_1^{\text{I}}\right) + \frac{n_1}{n_2}\left(\phi_2^{\text{II}} - \phi_2^{\text{I}}\right)}{n_1\left(\left(\phi_2^{\text{II}}\right)^2 - \left(\phi_2^{\text{I}}\right)^2\right)} \quad (4)$$

Equation 4 allows for a direct determination of the interaction parameter via composition measurements of the phase-separated blend. For composition analysis, fully phase separated binary blends are removed from the oven and cooled to room temperature rapidly (20 seconds) to capture the compositions of the coexisting phases in the melt. After cooling, the composition of the upper phase is determined by either FTIR or NMR.

Figs 4 and 5 show representative NMR and FTIR spectra used for composition measurements, respectively. If the overall blend composition and the composition of one phase are known, the composition of the remaining phase is determined via mass balance. Infrared analysis was useful for composition analysis

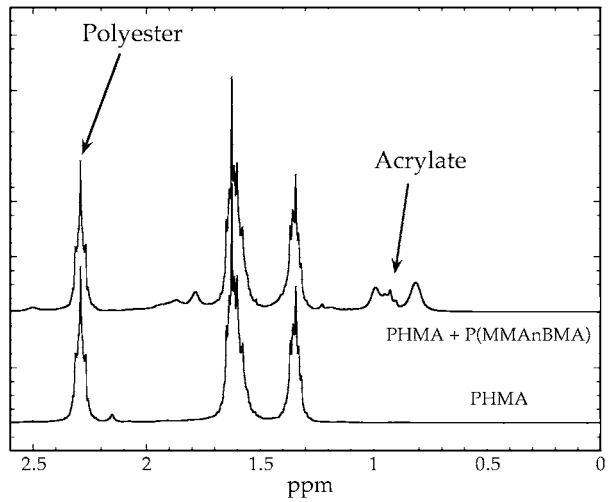

Figure 4 Example ^{1}H-NMR spectra used for composition determination of phase separated polyester, acrylic co-polymer binary blends.

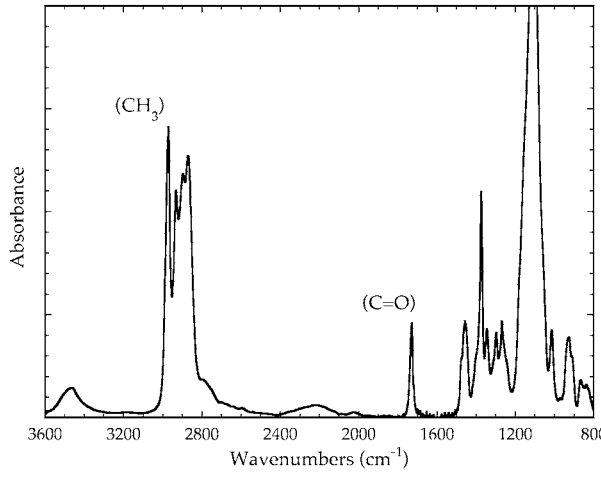

Figure 5 Example of FTIR spectra used for composition determination of phase separated polyether, polyester binary blends.

TABLE II Interaction parameters and interaction energy densities

Binary blend	g (critical)	g (exp)	B (kJ/m^3)
PPG/PHMA	0.053	0.0647[a]	3684
PPG/PHMS	0.056	−0.0325[b]	−1591
PPG/Acrylic	0.024	0.0272[a]	1548
PHMA/Acrylic	0.019	0.0233[a]	1326
PHMS/Acrylic	0.021	0.0286[a]	1628

[a]Composition analysis, 120°C.
[b]Melting point depression, 55 to 65°C.

of the PPG/PHMA and PPG/P(MMA*n*BMA) blends due to characteristic and cleanly resolvable methyl and carbonyl vibrations at 2973 and 1735 cm^{-1} respectively. The composition of PHMA/P(MMA*n*BMA) and PHMS/P(MMA*n*BMA) blends was more readily obtained using NMR. Resonances between 0.7 and 1.1 ppm were used for the P(MMA*n*BMA) population and resonances centered at 2.35 ppm were used for the PHMA and PHMS populations. A series of infrared and NMR spectra of known composition were recorded and used to construct calibration curves. The measured compositions are then used to calculate the interaction constants listed in Table II.

The remaining binary blend (PPG/PHMS) is miscible for all compositions. In this case, it is impossible to determine interaction parameters using the approach described above. For miscible blends interaction parameters can be obtained using cloud point data [30] or thermal analysis [33]. Melting point depression will be used to obtain the interaction parameter in this case. Equation 5 presents a relationship between the melting point depression and binary interaction parameter [33].

$$\left(\frac{1}{T_m} - \frac{1}{T_m^0}\right) = \frac{-g_{1,2} R V_{2u}}{\Delta H_{2u} V_{1u}} \phi_1^2 \qquad (5)$$

where T_m is the melting point of the blend and T_m^0 is the melting point of component 2 in K. V_{1u} and V_{2u} are the molar volumes per repeat unit of the two components. ΔH_{2u} is the enthalpy of fusion of component 2 per mole repeat unit, $g_{1,2}$ is the interaction parameter, ϕ_1 is the volume fraction of component 1, R is the gas constant. Using $T_m^0 = 337.75$ K (64.6°C), $V_{1u} = 57.4$ cm^3/mol, $V_{2u} = 277.6$ cm^3/mol, $\Delta H_{2u} = 26.14$ kJ/mol and the melting point depression in Fig. 6 we obtain an interaction parameter of –0.0325 as listed in Table II. The interaction energy density B defined as $(g_{1,2} RT/V_{1u})$ is sometimes used rather than g, values of B have been included in Table II for comparison purposes. It should be noted that one of the interaction constants (PPG/PHMS) was determined at lower temperatures because the melting point depression method was used. In this case, we found this pair to be miscible for all compositions.

Two aspects of the interaction constants are of interest. First, how do these compare to others observed for similar polymer systems? Second, how do the simulated ternary phase diagrams compare to experimental observations? Of additional interest is the critical interaction parameter (g^{crit}), given by Equation 6. It represents the largest g value that a binary blend may have while exhibiting complete miscibility. The g_{ij} values obtained

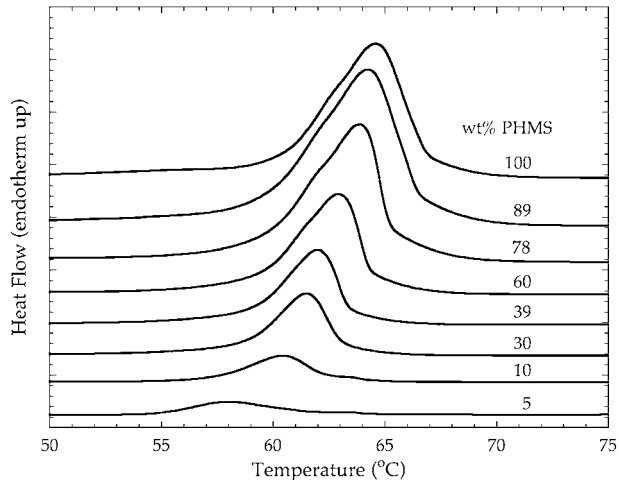

Figure 6 Thermal data for PPG/PHMS binary blends used for interaction parameter determination. The weight percent of PHMS in each blend is denoted in the figure.

are not significantly larger than obtained g_{crit} values. This is consistent with the fact that partial miscibility is associated with the blends studied and is in contrast to previous studies of highly incompatible blends [34]. In that case, the experimental interaction parameter was 0.449 compared to a critical value of 0.001.

$$g_{1,2}^{\text{critical}} = \frac{1}{2}\left(n_1^{-\frac{1}{2}} + n_2^{-\frac{1}{2}}\right)^2 \qquad (6)$$

The spinodal conditions for binary and ternary blends are given in Equations 7a and 7b respectively [21, 35].

$$\frac{1}{n_1\phi_1} + \frac{1}{n_2(1-\phi_1)} - 2g_{1,2} = 0 \qquad (7a)$$

$$\left(\frac{1}{n_1\phi_1} + \frac{1}{n_3\phi_3} - 2g_{1,3}\right)\left(\frac{1}{n_2\phi_2} + \frac{1}{n_3\phi_3} - 2g_{2,3}\right) - \left(\frac{1}{n_3\phi_3} + g_{1,2} - g_{2,3} - g_{1,3}\right)^2 = 0 \qquad (7b)$$

For binary blends Equation 7a can be solved exactly. Equation 7b was numerically evaluated to determine the stability boundaries for the ternary blends. If the left-hand-side of Equation 7b is <0 the composition is unstable, otherwise it is stable or metastable. The binodals were calculated using a numerical procedure adapted from a previous study [36]. Briefly, initial composition ϕ_0 within the spinodal region is allowed to form two coexisting phases I and II with overall compositions ϕ_I and ϕ_{II} with relative phase fractions Γ_I and Γ_{II}. The compositions and the relative phase fractions of the two co-existing phases are iterated until the free energy of the two coexisting phases is a minimum with respect to the free energy of the initial composition.

Fig. 7 illustrates the location of the phase boundaries for the four immiscible binary blends in the melt at 120°C. These four binary free energy functions represent the behavior of the blends on the edges of the ternary phase diagrams, Figs 2 and 3. The free energy functions are very similar for the PHMA/P(MMA*n*BMA) and PHMS/P(MMA*n*BMA)

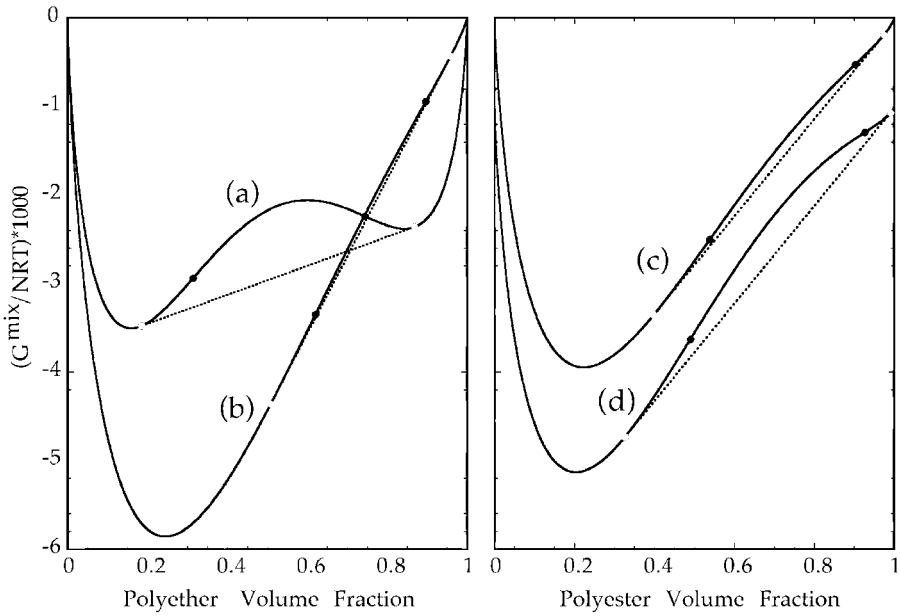

Figure 7 Free energy of mixing for the four immiscible binary polymer pairs. (a) PPG/PHMA, (b) PPG/P(MMA*n*BMA), (c) PHMA/P(MMA*n*BMA) and (d) PHMS/P(MMA*n*BMA). Open circles and dotted lined represent binodals, filled circles spinodals.

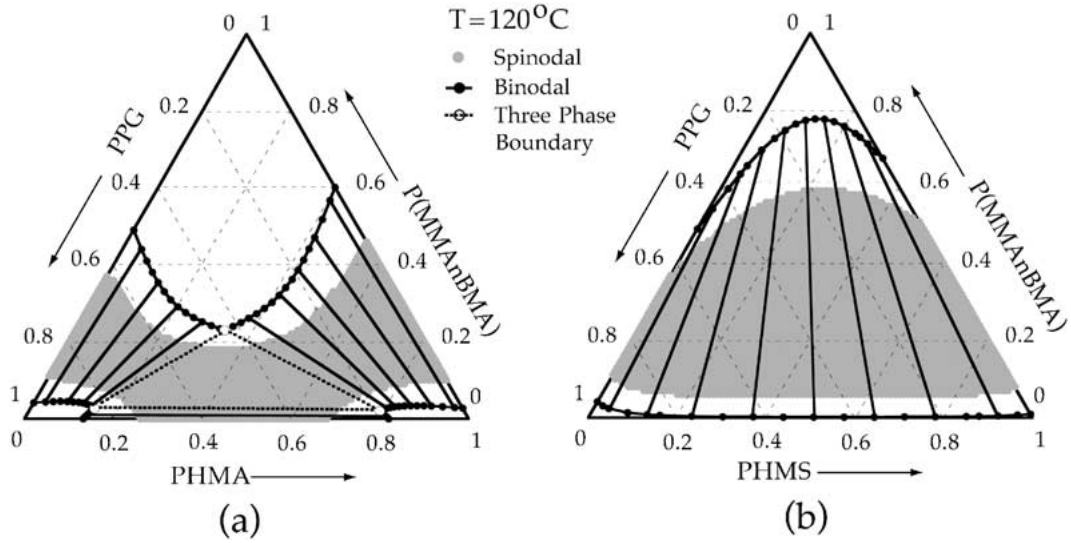

Figure 8 Calculated phase diagram for (a) PPG/PHMA/P(MMA*n*BMA) ternary blends and (b) PPG/PHMS/P(MMA*n*BMA) ternary blends at 120°C.

binary blends. The change in the aliphatic structure does not have the same effect as on the polyether/polyester binaries. The PPG/P(MMA*n*BMA) binary remains invariant with respect to the aliphatic polyester structure. These results suggest that different ternary phase behaviors originate in the PPG/PHMS and PPG/PHMA binary interactions.

The phase diagram for the PPG/PHMA/P(MMA*n*BMA) ternary system calculated from the binary interaction parameters is shown in Fig. 8a. This phase diagram shows three regions where the stability-function is positive, separated by a continuous unstable region. There are three single phase regions, three two phase regions and one three phase region. The two-phase regions are adjacent to the three binary axes. The triangular region within the two-phase regions is a three-phase region. The observed optical states of the blends in Fig. 2 are in reasonable agreement with the phase boundaries calculated from the binary interaction model in Fig. 8a. Although all three binaries are partially miscible, a large region of miscibility is found.

Fig. 8b shows the phase boundaries calculated for the PPG/PHMS/P(MMA-*n*BMA) ternary blends. This system contains two single phase and one large two-phase region. The single phase regions are located at low acrylic content (<1 wt%) and for acrylic contents >65 wt%. It should be noted that the miscible region containing low acrylate content abuts the PPG/PHMS axis and is difficult to observe. The phase boundaries shown in Fig. 8b appear in good agreement with the observed behavior in Fig. 3, indicating that the phase behavior of the PPG/PHMS/P(MMA*n*BMA) ternary blends is reasonably well reproduced using the binary interactions adopted here. Two of the binaries are partially miscible in this system. Although the PPG/PHMS binary is miscible, this did not translate into a wider range of miscibility in the ternary system.

Miscibility diagrams and interaction parameters of both types of ternary systems have been determined. The question of how the balance of interaction parameters is different in the two systems and the relationship with the polyester structure remains for discussion. The PPG/PHMA and PPG/PHMS binary blends are the most dramatically affected by the structural change in the polyester. Comparing the degree of polymerization in Table I, the molecular weight difference between PHMS and PHMA is not sufficiently large to cause such a dramatic change. Both PHMA and PHMS are terminated with primary OH groups. Since the molecular weight of the two polymers is similar, the same number of OH groups should be present in each system. For this system, contributions from end groups, specific interactions and molecular weight do not appear to be driving forces for miscibility. The primary difference between PHMA and PHMS is the length of the methylene chain between the carbonyl groups as shown in Fig. 1. The longer methylene segment changes the periodicity of the carbonyl groups in PHMS. The effect of chain length on aliphatic polyester miscibility is characteristic of this family of polymers [9, 10, 17–19].

The appearance of miscible and immiscible regions in ternary blends with two and three miscible binaries has been reported [37]. In many cases the phase behavior is attributed to the relative magnitudes of the three binary interaction parameters, sometimes referred to as the $\Delta\chi$ effect [37]. The asymmetry, difference in size and sign of the interaction parameters, can lead to immiscible regions in systems composed of three miscible binary polymers [38]. For a ternary system with one solvent, component 1, and two polymers, components 2 and 3, $|\Delta\chi|$ is given by $|\chi_{12} - \chi_{13}|$, the difference between the two polymer solvent interactions. The polymer–polymer interaction χ_{23} will dominate if $|\Delta\chi|$ is small. If P(MMA*n*BMA) is treated as solvent, the interaction between polyether and polyesters is far larger than any difference between polyether/acrylate or polyester/acrylate systems. In the context of the $|\Delta\chi|$ effect these systems seem dominated by the polymer–polymer interaction χ_{23} not by the difference in polymer–solvent interactions $|\Delta\chi|$.

The treatment of copolymer interaction parameters provides a possible explanation for the observed miscibility behavior of the PPG/PHMA and PPG/PHMS binary blends. For a binary blend of copolymers AB and CD [11].

$$\begin{aligned}\chi_{\text{blend}} = {} & \chi_{\text{A,C}}xy + \chi_{\text{A,D}}x(1-y) + \chi_{\text{B,C}}(1-x)y \\ & + \chi_{\text{B,D}}(1-x)(1-y) - \chi_{\text{A,B}}x(1-x) \\ & - \chi_{\text{C,D}}y(1-y) \end{aligned} \quad (8)$$

The volume fraction of A in AB is (x) and of C in CD is (y). Six interaction terms appear in Equation 8, four interactions between segments on different chains and two for the interactions between units on the same chain. If PHMA and PHMS are treated as co-polymers of CH_2 and COO units and PPG a homopolymer, Equation 8 can then be rewritten as

$$\chi_{\text{blend}} = \chi_{\text{A,D}} + (\chi_{\text{A,C}} - \chi_{\text{A,D}} - \chi_{\text{C,D}})y + \chi_{\text{C,D}}y^2 \quad (9)$$

C and D represent the CH_2 and COO groups of the polyesters and A represents the poly(propylene oxide) homopolymer. The interaction parameter for the blend will depend on the CH_2 and COO composition (y) and will have a minimum or maximum depending on the sign of (χ_{CD}) [11]. Ellis reported a value of 2.223 for the segmental interaction parameter of CH_2 with COO groups. It was argued that this interaction is important in consideration of blends involving different aliphatic polyesters [10]. This line of reasoning has also been considered in the explanation of miscibility windows observed for blends of aliphatic polyesters with poly(vinyl chloride) [17], tetramethyl bisphenol-A polyarylate [9], phenoxy [15, 19] and poly(epichlorohydrin) [18].

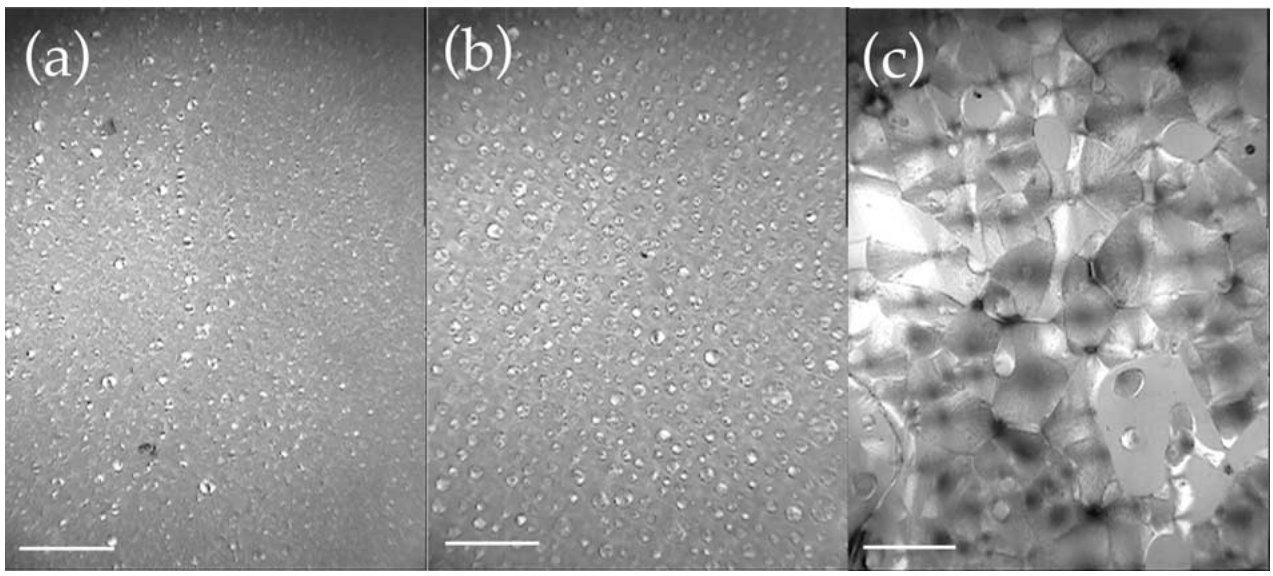

Figure 9 Optical micrographs of ternary PPG/PHMA/P(MMA*n*BMA) blends cooled from the melt blends with different locations in the phase diagram. The compositions of the blends are (a) (40, 30, 30), (b) (70, 20, 10) and (c) (20, 60, 20). [PPG, PHMA, P(MMA*n*BMA)] wt% Scale bar = 500 μm.

The results presented above suggest molecular interpretations of phase behavior and possibly improvements in morphological and mechanical properties. Changing the chemical structure of the polyester repeat unit has a dramatic effect on the miscibility behavior of the PPG/PHMA and PPG/PHMS binary blends as shown in Figs 2, 3 and 8. The next important aspect to understand is how miscibility behavior translates into morphological differences in the blends. Fig. 9 shows micrographs of three ternary PPG/PHMA/P(MMA-BMA) blends representative of blends located in different regions in the ternary phase diagram after being cooled from the melt. The ternary blend in Fig. 9a lies near the center of the composition triangle above the binodal shown in Fig. 8a, indicating that it is stable in the melt. The blend in Fig. 9b is from the lower left, poly(propylene oxide) rich corner of the composition triangle in a two-phase unstable region bordering the three phase region. The blend in Fig. 9c is located in the lower right PHMA rich corner also within a two-phase unstable region, but further from the three phase region than the blend shown in Fig. 9b. All three blends appear heterogeneous due to crystallization of the polyester component. Upon cooling from the melt, the ternary system begins a transition from liquid–liquid to liquid–solid and finally solid-solid equilibrium. When cooled, the PHMA crystallizes. The morphology formed is notably different amongst the blends and depends on composition. The size and number of the crystallites formed govern melt viscosity. The degree of compatibility between the crystallizable polymer and the amorphous polymer has a strong influence on the morphology and crystallization kinetics [33, 39]. The tie lines in Figs 8a and b predict the composition of the coexisting phases. This information could be used to rationally design and control morphologies of multicomponent blends.

4. Conclusions

Changes in the structure of the aliphatic polyester repeat unit have been shown to change the miscibility behavior of PHMA and PHMS with PPG in the melt. PPG/PHMS binary blends were found to be miscible and PPG/PHMA blends immiscible in the melt. The optical states of ternary PPG/PHMA/P(MMA*n*BMA) and PPG/PHMS/P(MMA*n*BMA) blends were measured. The miscibility of PPG with PHMA and PHMS has a large impact on the phase behavior of the ternary blends.

We have presented a method based on direct composition measurements of co-existing phases that allows for determination of binary interaction parameters of partially miscible polymer blends. The binary interaction parameters are used to calculate spinodals and binodals of the ternary systems, defining regions of stability. The calculated phase behavior is found to be in good agreement with experimental miscibility maps.

The culmination of the thermodynamic analysis presented here is the ability to correlate morphological differences in Fig. 9 to the stability of the polymer blend in the melt shown in Figs 8a and b. Optical micrographs of the phase-separated systems offer a simple way to illustrate the range of morphologies that can be obtained for immiscible systems. Knowing the location of these boundaries is valuable because the method of blend decomposition can affect the final morphology of a polymer blend in the melt or when cooled. The change in the miscibility behavior is attributed to the difference in the polyester structure.

References

1. R. DE GENOVA, M. D. HARPER, W. A. CLAY, P. E. CRANLEY and M. K. HUNTER, *TAPPI J.* **79** (1996) 196.
2. R. DE GENOVA, L. GRIER, P. MURRAY and W. CLAY, *TAPPI J.* **6** (1998) 196.
3. W. F. GUM, W. RIESE and H. ULRICH (eds.) "Reaction Polymers: Chemistry, Technology, Applications , Markets" (Hanser, Munich, Vienna, New York, Barcelona, 1992) p. 838.
4. L. A. UTRACKI, in "Commercial Polymer Blends" (Chapman and Hall, London, 1998) p. 658.
5. D. BRAUN, D. YU, L. N. ANDRADI, B. LOWENHAUPT and G. P. HELLMANN, *Makromol. Chem. Makromol. Symp.* **48/49** (1991) 55.
6. S. DATTA and D. J. LOHSE, in "Polymeric Compatibilizers: Uses and Benefits in Polymer Blends" (Hanser, Munich, Vienna, New York, 1996) p. 542.
7. M. J. GALANTE, J. BORRAJO, R. J. J. WILLIAMS, E. GIRARD-REYDET and J. P. PASCAULT, *Macromolecules* **34** (2001) 2686.
8. K. I. WINEY, M. L. BERBA and M. E. GALVIN, *ibid.* **29** (1996) 2868.
9. T. O. AHN, M. LEE, H. M. JEONG and K. CHO, *J. Polym. Sci. B Polym. Phys.* **36** (1998) 201.
10. T. S. ELLIS, *Macromolecules* **28** (1995) 1882.
11. R. J. ROE and D. RIGBY, *Adv. Polym. Sci.* **82** (1987) 103.
12. Z. CHAI, R. SUN, S. LI and F. E. KARASZ, *Macromolecules* **28** (1995) 2297.
13. G. BEAUCAGE, R. S. STEIN and R. KONINGSVELD, *ibid.* **26** (1993) 1603.
14. M. H. LEE, C. A. FLEISCHER, A. R. MORALES, J. T. KOBERSTEIN and R. KONINGSVELD, *Polymer* **42** (2001) 9163.
15. M. M. COLEMAN, X. YANG, P. C. PAINTER and J. F. GRAF, *Macromolecules* **25** (1992) 4414.
16. M. M. COLEMAN and P. C. PAINTER, *Prog. Polym. Sci.* **20** (1995) 1.
17. E. M. WOO, J. W. BARLOW and D. R. PAUL, *Polymer* **26** (1985) 763.
18. A. C. FERNANDES, J. W. BARLOW and D. R. PAUL, *J. Appl. Polym. Sci.* **29** (1984) 1971.
19. J. E. HARRIS, S. H. GOH, D. R. PAUL and J. W. BARLOW, *ibid.* **27** (1982) 839.
20. Y. HU, P. C. PAINTER and M. M. COLEMANN, *ibid.* **70** (1998) 1265.
21. R. KONINGSVELD, W. H. STOCKMAYER and E. NIES, in "Polymer Phase Diagrams: A Textbook" (Oxford University Press, New York, 2001) p. 341.
22. C. C. HSU and J. M. PRAUSNITZ, *Macromolecules* **7** (1974) 320.
23. P. A. SMALL, *J. Appl. Chem.* **3** (1953) 71.
24. R. N. FRENCH, J. M. WALSH and J. M. MACHADO, *Polym. Eng. Sci.* **34** (1994) 42.
25. R. LAGO, P. J. ORTIZ and R. MARTINEZ, *Acta Polym.* **42** (1991) 403.
26. O. OLABISI, L. M. ROBESON and M. T. SHAW, in "Polymer–Polymer Miscibility" (Academic Press, New York, London, Toronto, Sydney, San Francisco, 1979) p. 370.
27. A. C. SU and J. R. FRIED, *Polym. Eng. and Sci.* **27** (1987) 1657.
28. M. HOSOKAWA and S. AKIYAMA, *Polym. J.* **31** (1999) 13.
29. J. A. POMPOSO, M. CORTAZAR and E. CALAHORRA, *Macromolecules* **27** (1994) 252.
30. S. VANHEE, R. KONINGSVELD and H. BERGHMANS, *ibid.* **33** (2000) 3924.
31. A. ZIVNY and J. POUCHLY, *J. Polym Sci. Part A2* **10** (1972) 1467.

32. W. Y. CHUANG, T. H. YOUNG, D. M. WANG, R. L. LUO and Y. M. SUN, *Polymer* **41** (2000) 8339.
33. T. NISHI and T. T. WANG, *Macromolecules* **8** (1975) 909.
34. H. M. PETRI, R. HORST and B. A. WOLF, *Polymer* **37** (1996) 2709.
35. J. A. POMPOSO, E. CALAHORRA, I. EGUIAZABAL and M. CORTAZAR, *Macromolecules* **26** (1993) 2104.
36. R. HORST, *J. Phys Chem. B* **102** (1998) 3243.
37. G. R. BRANNOCK and D. R. PAUL, *Macromolecules* **23** (1990) 5240.
38. M. RABEONY, D. B. SIANO, D. G. PEIFFER, E. SIAKALI-KIOULAFA and N. HADJICHRISTIDIS, *Polymer* **35** (1994) 1033.
39. T. K. KWEI, G. D. PATTERSON and T. T. WANG, *Macromolecules* **9** (1976) 780.

Received 28 March
and accepted 28 May 2002